

Evaluation of local field effect on the ${}^4I_{13/2}$ lifetimes in Er-doped silica-hafnia planar waveguides

L. Zampedri,* M. Mattarelli, and M. Montagna

Dipartimento di Fisica, CSMFO Group, Università di Trento, Via Sommarive 14, I-38050 Trento, Italy

R. R. Gonçalves

Departamento de Química, Faculdade de Filosofia, Ciências e Letras de Ribeirão Preto, Universidade de São Paulo, Avenida Bandeirantes 3900, Monte Alegre 14040-901, Ribeirão Preto, São Paulo, Brazil

(Received 11 July 2006; published 27 February 2007)

A series of $(100-x)$ SiO₂- x HfO₂ planar waveguides ($10 < x < 45$) doped with 0.01 mol % Er³⁺ was prepared by a sol-gel route. The lifetime of the ${}^4I_{13/2}$ level and the refractive index of the waveguides were measured. The magnetic dipole and electric dipole rates of the ${}^4I_{13/2} \rightarrow {}^4I_{15/2}$ transition were estimated as a function of the refractive index. The electric dipole transition rates were well reproduced by the real cavity model.

DOI: 10.1103/PhysRevB.75.073105

PACS number(s): 42.82.Et, 42.70.Ce, 32.70.Cs, 71.20.Eh

The spontaneous emission (SE) rate (Γ_0) of the free atom in vacuum is due to the interaction of the free ion with the electromagnetic vacuum fluctuation.¹ When the atom is embedded in a medium, the SE rate suffers a modification because of the changes in the density of electromagnetic states and because of the electromagnetic fields generated by the other atoms in its neighborhood. In an inhomogeneous system containing interfaces, mirrors, and cavities, the two effects cannot be easily separated. However, in a homogeneous system described by the refractive index n , the density of electromagnetic states simply increases by a factor of n^3 with respect to the vacuum level. In the past few years, a lot of theoretical and experimental papers have been focused on the study of the local field effect on emitting ions embedded in dielectric media.²⁻⁸ In an absorption process, the total electromagnetic field, consisting of the sum of the electric field of the incident light E_{light} and the electric field of the dipole induced by the presence of other atomic species E_{dip} , is called the effective field E_{eff} ($E_{eff} = E_{light} + E_{dip}$). All these effects produce a modification of the decay rate that may be expected to be modified to

$$\Gamma_{eff} = nf(n)\Gamma_0, \quad (1)$$

where $f(n)$ is the local field correction factor and n is the refractive index of the medium.^{2,6} Two different models have been proposed for the $f(n)$ factor: (i) the virtual cavity model⁹ (VCM) and (ii) the real cavity model (RCM).¹⁰ In both cases, it has been assumed that the emitting object is located inside a spherical cavity of radius r , where r is large compared to the linear size of the emitting object, but much smaller than the radiation wavelength. In the VCM, based on the work of Lorentz, it is assumed that the emitting ion is at the center of a cavity filled with a medium with the same dielectric constant as the surrounding environment, obtaining

$$f(n) = \left(\frac{n^2 + 2}{3} \right)^2. \quad (2)$$

The RCM, developed by Glauber and Lewenstein,¹⁰ assumed that the emitting ion is inside a real empty spherical cavity in the dielectric and leads to

$$f(n) = \left(\frac{3n^2}{2n^2 + 1} \right)^2. \quad (3)$$

There is a general agreement that local field effects are not present for magnetic dipole (MD) transitions in dielectrics, where the magnetic susceptibility equals the vacuum value.¹¹ Therefore, for MD transitions, only the n^3 dependence of the density of states will affect the radiative rates, in homogeneous media. The modification of the SE rate has been experimentally shown for Eu³⁺ ions in different materials such as in a dense supercritical gas,⁶ in PbO-B₂O₃,⁷ in Y₂O₃,⁴ and in hfa-topo complex.¹¹ Some investigators have studied the modification of the spontaneous emission rate of the ${}^4I_{13/2}$ level of Er³⁺ ions in different materials.^{8,12,13} Most experimental results seem to indicate that the real cavity model is favored for the electric dipole (ED) transitions.^{6,7,11}

The refractive index of the medium is not the only parameter that governs the transitions rates. In fact, all $f-f$ transitions are electric dipole forbidden if the rare earth is located in sites with inversion symmetry, so that the electronic wave functions have defined parity. Parity mixing is produced by odd parity distortions of the crystal field. For the study of the dependence of the transition rates on the refractive index in solids, these local effects are problematic. In fact, when n changes due to a change of the glass composition, the local structure and the distribution of the crystal field also change. The crystal field at the active ions is usually studied by applying the Judd-Ofelt theory.¹⁴ From the measured absorption cross sections of many excited states, the odd distortions of the crystal field are estimated by using three parameters, allowing one to calculate all ED transition rates between pairs of states and lifetimes of the excited levels. However, the method needs an estimation of the local field effect. This is usually done by using Eq. (2). The transition rates in different host media show a large distribution of values, which are related mainly to the different crystal fields, even if the local field effect also plays an important role.¹⁵⁻¹⁷ Therefore, it is very dangerous to assign all the observed changes of the lifetimes to changes of the effective field through n without considering that important effects could be due to changes of the crystal field associated with a change of the structure, which also changes the refractive index. Recently, the avail-

TABLE I. Optical and spectroscopic parameters of the 0.01 mol % Er³⁺-activated SiO₂-HfO₂ planar waveguides.

Label	W10	W20	W25	W30	W35	W40	W45
mol % HfO ₂	10	20	25	30	35	40	45
Thickness (μm)	1.16	0.69	0.67	0.69	0.60	0.53	0.45
<i>n</i> at 543.5 nm	1.497	1.566	1.574	1.611	1.638	1.670	1.716
<i>n</i> at 632.8 nm	1.494	1.562	1.565	1.605	1.632	1.664	1.709
<i>n</i> at 1.55 μm	1.476	1.543	1.550	1.586	1.612	1.643	1.687
Lifetimes (ms)	8.5	7.5	7.4	7.0	6.8	6.6	6.3
FWHM (nm)	50	50	51	50	50	49	48

able experimental data on the subject have been critically reviewed.¹⁸ Meltzer *et al.* and Wuister *et al.* found a good strategy for dividing the two effects by dissolving active nanocrystals in media with different refractive indices.^{4,5} Our strategy, in this work, is to study a series of glasses with different HfO₂/SiO₂ ratios, covering a wide range of the refractive index, whereas the local structure around an erbium ion does not change significantly.

The glassy waveguides were produced by a sol-gel route using the dip coating deposition procedure. The starting solution has been obtained using tetraethylorthosilicate, ethanol, de-ionized water, hydrochloric acid, an ethanolic colloidal suspension of HfOCl₂, and Er(NO₃)₃·5H₂O. The quantity of Er³⁺ ions has been fixed to 0.01 mol %. We have prepared solutions with different Si/Hf molar ratios: 55/45, 60/40, 65/35, 70/30, 75/25, 80/20, and 90/10. Erbium-activated silica-hafnia films were deposited on silica substrates by dip coating; the annealing temperature between the single deposition has been chosen at 900 °C. Finally, the waveguides were submitted to a further annealing at 900 °C for the time necessary to produce full densification, depending on the Si:Hf ratio. An exhaustive description of the preparation and deposition procedure is reported elsewhere.^{19,20} Table I shows the composition and thickness of the prepared waveguides. As a result of the procedure, transparent and crack-free waveguides were obtained.

The thickness of the waveguides and the refractive index at 543.5, 632.8, and 1530 nm were measured with a m-line apparatus based on the prism coupling technique.²¹ For waveguides with low confinement coefficient at 1530 nm, the *n* value obtained by extrapolation from the visible measurements was preferred to the measured one. The TE₀ mode waveguiding excitation was used for photoluminescence measurements, detecting the luminescence from the front of the waveguide. Photoluminescence measurements in the region of the ⁴I_{13/2} → ⁴I_{15/2} transition of Er³⁺ ions were performed using the 980 nm line of a titanium sapphire laser and the 514.5 nm line of an argon laser as excitation source and dispersing the luminescence with a 320 mm single-grating monochromator with a resolution of 2 nm. The light was detected using an InGaAs photodiode and standard lock-in technique. Decay curves were obtained by chopping the cw exciting beam with a mechanical chopper and recording the signal with a digital oscilloscope. All the measurements were performed at room temperature. All waveguides

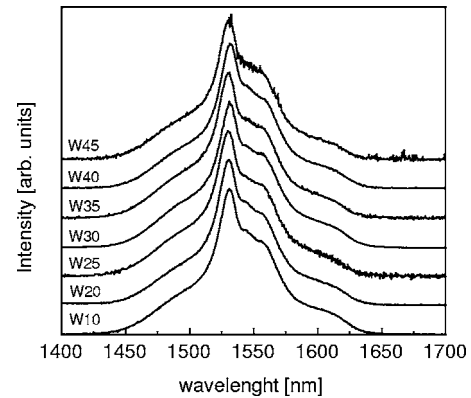


FIG. 1. Photoluminescence spectra relative to the ⁴I_{13/2} → ⁴I_{15/2} transition of the Er³⁺ ions for the planar waveguides upon 514 nm excitation.

support two TE and two TM modes at 543.5 nm and have a refractive index ranging from 1.497 to 1.716 depending on the Si/Hf values (see Table I). Raman measurements do not show any vibration due to OH groups. This is important because the OH vibrations give a competitive nonradiative relaxation rate and furthermore the absence of the groups tied to the pore surface indicates that a high degree of densification has been achieved.²⁰

Figure 1 shows the normalized photoluminescence spectra of the waveguides. All spectra exhibit a main emission peak at 1.53 μm with a shoulder at about 1.55 μm and a full width at half maximum (FWHM) of about 50 nm. The shape of the emission spectrum at 1.5 μm and in the visible region, not reported here, does not change significantly with the hafnia concentration, indicating that there are no important changes in the local structure around the erbium ions even by increasing the hafnia concentration from 10 to 45 mol %. This is surprising since the structure of the glass does, in fact, change quite significantly with the HfO₂ content and the FWHM in silica is about one-half of those observed here. Extended x-ray-absorption fine structure measurements at the erbium edge show that the short-range structure (first and second coordination shells) is practically independent of the hafnia concentration.²² The picture that seems to emerge is that a spinodal separation of the two phases occurs, as already observed in silica-zirconia glasses.^{23,24} The erbium ions are concentrated in the hafnia rich regions, and this explains why its local environment does not dramatically depend on the glass composition. Therefore, we expect that the composition dependence of the local structure plays a minor role in the studied system so that the changes of the rates of the radiative transitions are mainly governed by changes in the refractive index. Furthermore, the use of the macroscopic *n* value for evaluating the effective field is justified, since the size of the compositional fluctuation in the glass is of the order of 10 nm, much smaller than the wavelength of the light.²⁴ Finally, we need to consider possible effects of light confinement caused by the structure of the waveguides. Snoeks *et al.* measured the change in the lifetime of erbium ions implanted near a glass surface, when the films are covered with liquid having different *n* values.⁸ From their experimental results and their calculation of the

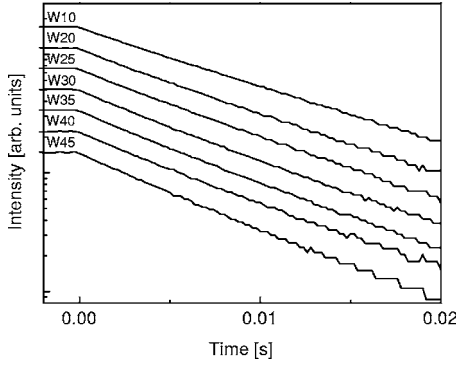


FIG. 2. Decay curves of the luminescence from the ${}^4I_{13/2}$ metastable state of Er^{3+} ions upon 514 nm excitation.

density of electromagnetic states in the film, we can expect that the average lifetime in the films with a thickness of about $1\ \mu\text{m}$, as those used in the present work, is very close to that of a bulk system. Moreover, the excitation was performed in a guided configuration (TE_0 mode), where the emitting ions are mostly confined to the middle of the waveguides. The fact that no change in the decay trace was observed changing the excitation wavelength from 514.5 to 980 nm (the second less confined than the first) strongly supports our consideration.

Figure 2 shows the decay curve of the ${}^4I_{13/2}$ metastable state obtained upon 514 nm excitation. All the curves can be fitted by a single exponential function and lifetimes ranging between 8.5 and 6.3 ms have been obtained (Table I).

The total transition rate (Γ_{tot}) can be considered as a sum of different contributions:

$$\Gamma_{\text{tot}} = A_{\text{rad}} + A_{\text{ET}} + A_{\text{phonon}}, \quad (4)$$

where A_{rad} is the radiative transition probability, A_{ET} is the transition probability related to the energy transfer processes, and A_{phonon} is the transition probability related to the multiphonon relaxations. In the hypothesis of a spatially homogeneous distribution of the active ions and for an Er^{3+} concentration of 0.01 mol %, the average distance between two ions is of the order of 7 nm. As the dipole-dipole interaction between a donor ion and an acceptor ion scales as $1/R^6$, where R is the distance between the two ions, we can assume that the A_{ET} is negligible.²⁵ As far as the multiphonon relaxation contribution is concerned, Layne *et al.* have estimated that the multiphonon decay rate is around $A_{\text{phonon}} = 0.5\ \text{s}^{-1}$ for silicate glasses with an energy gap of about $6500\ \text{cm}^{-1}$.²⁶ This value is negligible with respect to the radiative transition probability, which is of the order of $(0.007\ \text{s})^{-1} \approx 140\ \text{s}^{-1}$. Furthermore, in a HfO_2 environment, the nonradiative relaxations are expected to be even less efficient than in a silicate glass, since the phonon frequencies are smaller and a higher order of multiphonon transition is needed. It appears reasonable now that the lifetime measured in the samples doped with 0.01 mol % Er is really very close to the radiative lifetime in all the $(100-x)\ \text{SiO}_2-x\ \text{HfO}_2$ binary systems.

The optical transitions in Er^{3+} ions can be considered as pure ED transition, except for the ${}^4I_{13/2} \rightarrow {}^4I_{15/2}$ and for the

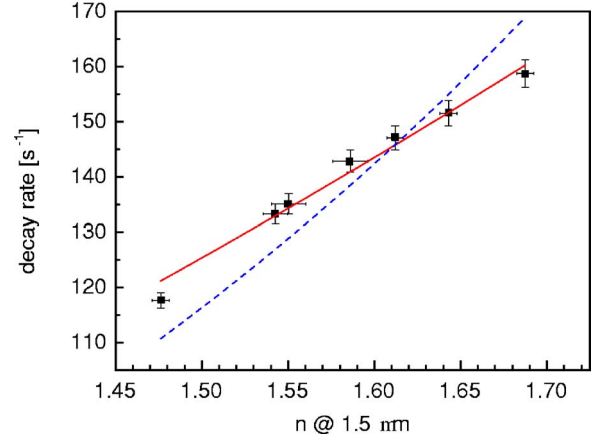


FIG. 3. (Color online) Decay rate of the ${}^4I_{13/2}$ level as a function of the refractive index at $1.55\ \mu\text{m}$. The data have been fitted with Eq. (6). Solid line: RCM with K and L as free parameters. Dashed line: VCM with K as a free parameter and $L = 10\ \text{s}^{-1}$.

${}^4I_{11/2} \rightarrow {}^4I_{13/2}$ transitions in which the magnetic dipole components become comparable with the electrical dipole ones.^{16,27} In general, we can write the total spontaneous transition rate between an initial J state and a final J' state as a sum of various contributions:²⁸

$$P(\Psi J; \Psi' J') = \frac{64\pi^4 e^2}{3\hbar(2J+1)\bar{\lambda}^3} [nf(n)S_{\text{ED}}(\Psi J; \Psi' J') + n^3 S_{\text{MD}}(\Psi J; \Psi' J')] = A_{\text{ED}} + A_{\text{MD}}, \quad (5)$$

where $\bar{\lambda}$ is the wavelength of the peak emission, n is the refractive index, $S_{\text{ED}}(\Psi J; \Psi' J')$ and $S_{\text{MD}}(\Psi J; \Psi' J')$ are the ED and MD line strengths, and A_{ED} and A_{MD} are the ED and MD transition probabilities. The function $f(n)$ is the local field correction factor.

Figure 3 shows the measured inverse lifetimes of the ${}^4I_{13/2}$ level as a function of the refractive index for the silica-hafnia planar waveguides. The data have been fitted using Eq. (5) in the following form:

$$P(\Psi J; \Psi' J') = Knf(n) + Ln^3, \quad (6)$$

with the two parameters K and L for the ED and MD transition rates.

In the case of the real cavity model, the fit gives $K = (39 \pm 2)\ \text{s}^{-1}$ and $L = (11.1 \pm 1.3)\ \text{s}^{-1}$ (solid line). It should be noted that the L value obtained by the fit coincides, within the experimental error, with the calculated one ($10\ \text{s}^{-1}$).^{15-17,27,29,30} On the contrary, the virtual cavity model cannot reproduce the data well. In fact, if both K and L are taken as free parameters, the best fit is obtained for a negative value of L . The dashed line of Fig. 3 is the fit to the virtual cavity model with only K as a free parameter and with fixed L to the calculated value, $L = 10\ \text{s}^{-1}$. In conclusion, we have prepared a set of fully densified silica-hafnia waveguides with different Hf/Si ratios ranging between 10/90 and 45/55 doped with very low (0.01%) Er^{3+} concentration. We have experimentally proven that the electric dipole transition rate is well reproduced by the real cavity

model. Further experimental data on different systems have to be collected to test the model. Note that the virtual cavity model has been used in hundreds of works in applying the Judd-Ofelt method for the calculation of the crystal-field effects on the ED transition rates. If the real cavity model will emerge as the best one, a lot of established data will need

revision. This effect would be more important for systems with high n , where the two models give divergent results.

The authors acknowledge M. Bettinelli for useful discussions, C. Armellini for technical support, and the financial support of MIUR-PRIN 2004.

*Corresponding author. FAX: +39-0461-881696. Email address: zampedri@science.unitn.it

¹P. Meystre and M. Sargent III, *Elements of Quantum Optics* (Springer, Berlin, 1998).

²S. Scheel, L. Knöll, D. G. Welsch, and S. M. Barnett, *Phys. Rev. A* **60**, 1590 (1999).

³S. Scheel, L. Knöll, and D. G. Welsch, *Phys. Rev. A* **60**, 4094 (1999).

⁴R. S. Meltzer, S. P. Feofilov, B. Tissue, and H. B. Yuan, *Phys. Rev. B* **60**, R14012 (1999).

⁵S. F. Wuister, C. de Mello Donega, and A. Meijerink, *J. Chem. Phys.* **121**, 1 (2004).

⁶F. J. P. Schuurmans, D. T. N. de Lang, G. H. Wegdam, R. Sprik, and A. Lagendijk, *Phys. Rev. Lett.* **80**, 5077 (1998).

⁷G. M. Kumar, D. N. Rao, and G. S. Agarwal, *Phys. Rev. Lett.* **91**, 203903 (2003).

⁸E. Snoeks, A. Lagendijk, and A. Polman, *Phys. Rev. Lett.* **74**, 2459 (1995).

⁹B. Di Bartolo, *Optical Interaction in Solids* (Wiley, New York, 1967).

¹⁰R. J. Glauber and M. Lewenstein, *Phys. Rev. A* **43**, 467 (1991).

¹¹G. L. J. A. Rikken and Y. A. R. R. Kessener, *Phys. Rev. Lett.* **74**, 880 (1995).

¹²J. Yang, S. Dai, Y. Zhou, L. Wen, L. Hu, and Z. Jiang, *J. Appl. Phys.* **93**, 977 (2003).

¹³Q. Chen *et al.*, *J. Non-Cryst. Solids* **324**, 12 (2003).

¹⁴K. A. Gschneidner, Jr. and L. Eyring, *Handbook on the Physics*

and Chemistry of Rare Earths (Elsevier, Amsterdam, 1998).

¹⁵H. Lin, S. Jiang, J. Wu, F. Song, N. Peyghambarian, and E. Y. B. Pun, *J. Phys. D* **36**, 812817 (2003).

¹⁶Y. G. Choi, K. H. Kim, and J. Heo, *J. Am. Ceram. Soc.* **82**, 2762 (1999).

¹⁷R. Rolli, M. Montagna, S. Chaussedent, A. Monteil, V. K. Tikhomirov, and M. Ferrari, *Opt. Mater. (Amsterdam, Neth.)* **21**, 743 (2003).

¹⁸C. K. Duan, M. F. Reid, and Z. Wang, *Phys. Lett. A* **343**, 474 (2005).

¹⁹R. R. Gonçalves *et al.*, *Appl. Phys. Lett.* **81**, 28 (2002).

²⁰L. Zampedri *et al.*, *J. Non-Cryst. Solids* **345–346**, 580 (2004).

²¹S. J. L. Ribeiro *et al.*, *Appl. Phys. Lett.* **77**, 3502 (2000).

²²N. D. Afify *et al.*, *Opt. Mater. (Amsterdam, Neth.)* **28**, 864867 (2006).

²³A. Gaudon, A. Dauger, A. Lecomte, B. Soulestin, and R. Guinebretire, *J. Eur. Ceram. Soc.* **25**, 283286 (2005).

²⁴G. Mountjoy *et al.*, *J. Sol-Gel Sci. Technol.* **26**, 161164 (2003).

²⁵S. Hüfner, *Optical Spectra of Transparent Rare Earth Compounds* (Academic, London, 1978).

²⁶C. B. Layne, W. H. Lowdermilk, and M. J. Weber, *Phys. Rev. B* **16**, 10 (1977).

²⁷S. Tanabe, *J. Non-Cryst. Solids* **256&257**, 282 (1999).

²⁸M. J. Weber, *Phys. Rev.* **157**, 262 (1967).

²⁹M. J. Weber, *Phys. Rev.* **171**, 283 (1968).

³⁰S. Tanabe and T. Hanada, *J. Non-Cryst. Solids* **196**, 101 (1996).